Electrical and Photoinduced Degradation of Polyfluorene Based Films and Light-Emitting Devices

V. N. Bliznyuk* and S. A. Carter

Physics Department, University of California Santa Cruz, Santa Cruz, California 95064

J. C. Scott, G. Klärner, R. D. Miller, and D. C. Miller

IBM Almaden Research Center, 650 Harry Road, San Jose, California 95120

Received June 8, 1998; Revised Manuscript Received November 6, 1998

ABSTRACT: Degradation-induced changes in the structural and optical properties of the polyfluorene-based blue emitting films and LEDs are examined using spectroscopic (FTIR, UV−vis, photo- and electroluminescence), analytical (FTIR and ESCA), and scanning probe microscopy techniques. The materials studied are oligomers (DP ∼ 10) of 9,9-di-*n*-hexylfluorene and its random copolymer with anthracene. In situ FTIR monitoring is used to characterize chemical changes in the active layer of operating LED devices. Two primary mechanisms of degradation are identified. In the first, photooxidation of the polymer matrix leads to the formation of an aromatic ketone, most likely fluorenone at the chain terminating monomer units, which quenches the fluorescence. The second process promotes aggregate formation, which then leads to loss of luminous intensity by exciton transfer and relaxation through excimers.

Introduction

Electroluminescence in conjugated polymers was discovered almost 10 years ago.[1] Polymer light emitting diodes (PLEDs) have attracted considerable interest because of their potential application in large-area light sources and flexible color displays with low power consumption.[2] It has been shown that the electroluminescence of PLEDs results from the radiative decay of singlet excitons formed by recombination of electron−hole pairs.[3,4] PLEDs offer potential advantages of low turn-on and operating voltages and light weight. They are flexible in their fabrication procedure as well as in the sense of their mechanical properties. The range of colors available from PLEDs now spans the entire visible spectrum. Blue-emitting polymers are of special interest because they are needed for the full gamut of color either in patterned RGB emitters or with the use of color converters.[5−7] A wide range of materials has been investigated and external efficiencies up to nearly 2% have been achieved.[8−10]

Although significant improvements in the stability of organic LEDs have been made,[11] device lifetime remains an issue for commercialization. For most applications, stable operation over several tens of thousands of hours is a requirement which has not yet been demonstrated for blue emitting PLEDs.[2,11] Photodegradation of phenylene vinylene derivatives has been shown to be mainly due to photooxidation[12,13] by either residual oxygen in the polymer itself or by that released from the indium−tin−oxide (ITO) electrode.[14] Identification of the mechanisms of conjugated polymer degradation continues to be an important issue, the understanding of which could improve the performance and lifetime of polymer-based devices.

Recently, polyfluorenes (PF)[15,16] were introduced as a prospective emitting layer for PLEDs. These materials display extremely high photoluminescence efficiencies both in solution and in solid films,[17−19] with emission wavelengths primarily in the blue spectral region. Their photostability and thermal stability are also found to be better than those of the phenylene vinylenes.[18] Nickel-mediated[20] coupling of arylene dihalides permits a wide variation in chemical structure and tunability of the emission wavelength. The synthetic technique is ideally suited to the preparation of substituted fluorene homo- and copolymers.

In this report we present a study of the degradation mechanisms of PLEDs based on two blue-emitting polyfluorene polymers. We have applied a combination of spectroscopic techniques, coupled with chemical and structural analysis. Chemical changes resulting from electrical degradation in operating diodes are examined by in situ Fourier transform infrared (FTIR) spectroscopy. Electrical degradation was also investigated by X-ray photoelectron spectroscopy (also known as electron spectroscopy for chemical analysis or ESCA). Changes in polymer film quality, thickness, and morphology were examined with atomic force microscopy (AFM).

Two primary modes of degradation are identified. In the first, which we term the chemical route, oxidation of the polymer matrix leads to the formation of an aromatic ketone, i.e., a carbonyl group, which quenches the fluorescence. The second process promotes physical aggregation which then leads to red-shifted fluorescence and reduced intensity by exciton migration and relaxation through excimers. We should emphasize that we use the term "aggregation" here in the sense of an assembly of partially aligned polymer chains and not necessarily as an assembly of chromophores with distinct optical features in ground-state absorption such as H- and J-aggregates.[21,22]

Experimental Methods

Synthesis. The synthesis of homo and copolymers of 9,9-di-*n*-hexyl-2,7-dibromofluorene monomers via the nickel(0)-mediated polymerization reaction (Yamamoto polymerization[20]) has been described previously.[18] Molecular weight control was achieved by the addition of 2-bromofluorene to the

10.1021/ma9808979 CCC: $18.00
Published on Web 12/22/1998

Chart 1

PDHF

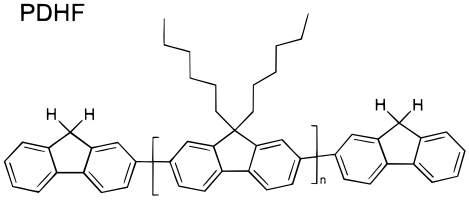

PDHF-15ANT

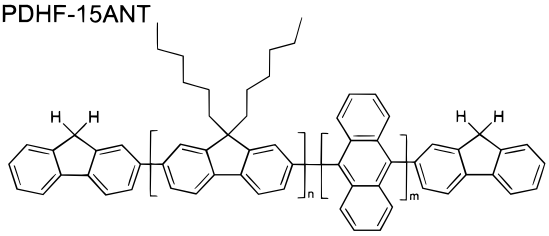

reaction, resulting in fluorene end-groups unsubstituted at the 9-position. A statistical copolymer from 9,9-di-*n*-hexyl-2,7-dibromofluorene and 9,10-dibromoanthracene, containing 15 mol. % anthracene units, was synthesized using a similar procedure.[19] The structures of the polymers studied are shown in Chart 1. We refer to these polymers as PDHF and PDHF−15ANT, respectively.

Standard techniques for purification, fractionation (HPLC), and characterization (^{1}H NMR) were used (see ref 18 for details). The molecular weights of the PF polymers were determined by gel permeation chromatography (GPC) using polystyrene standards. The number-average molecular weights of these polyfluorene derivatives corresponded to a degree of polymerization of order 10. The use of this lower molecular weight material represents a compromise between the need for polymer solubility in common organic solvents, good film forming properties, and the minimum chain length needed to obtain representative electronic properties. Previously, we have reported that the absorption and emission of PF derivatives are dependent on polymer chain length.[17] The effective conjugation length for absorption was determined to be ⩾12 monomer units for poly(di-*n*-hexylfluorene).

Sample Preparation. The diode devices used for in situ FTIR spectroscopy were fabricated on single crystal Si wafers ({111} orientation, undoped, polished both sides). The ITO anode, covering approximately two-thirds of the circular wafer, was deposited by reactive sputtering in Ar/N_2O at 3 mTorr partial pressure as described previously.[14] Typically an ITO thickness of 75 nm was used. The polymer layer, ca. 120 nm thick, was spin-coated on top of this electrode from a 30 mg/mL *p*-xylene solution at a spinning speed of 3000 rpm. The top aluminum cathode (50−75 nm) was deposited by vacuum evaporation. This electrode served also as a reflecting layer in the FTIR experiments. The emissive area of the devices (ca. 2.5 cm^2) is defined by the overlap of the ITO and the top metal electrode.

Films were also prepared on quartz substrates (for fluorescence and absorption spectroscopy) and gold-coated Si (FTIR study of photoinduced degradation). Thermally evaporated Au with a thickness of 100 nm was deposited on a 5 nm chromium underlayer for better adhesion to the Si surface. Solutions of PDHF in either *p*-xylene or 1,1,2,2-tetrachloroethane (TCE) at concentrations ranging from 2 to 60 mg/mL were used, and spinning speeds ranging from 1000 to 3000 rpm resulted in film thicknesses of 2.5−1500 nm. Slightly better optical quality films could be cast from TCE.

Photoinduced and Electrical Degradation. The photodegradation of polymer films on either silicon or quartz substrates was accomplished using a 365 nm UV lamp. The samples were irradiated with an intensity of 70 mW/cm^2 for up to 21 h. Several samples exposed, instead, at 254 nm gave similar results.

Electrical degradation was achieved by passing electrical current through a single layer diode device. For the usual

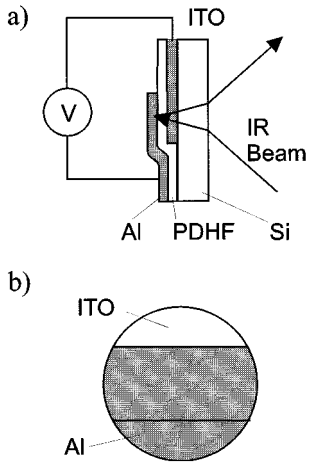

Figure 1. Diagram of the working PDHF device prepared for in situ FTIR experiments, where (a) is a cross section and (b) is a top view of the device.

device thicknesses of 100−150 nm, voltages up to 40 V were applied to drive a current of 0.001−0.1 A in forward bias or 10^{-7}−10^{-5} A in reverse bias. Typically, electrical degradation occurred rapidly after several minutes of operation. During this period, the current increased by up to an order of magnitude.

Absorption and Emission Spectroscopy. A Hewlett-Packard 8452 diode array spectrometer was used to record absorption spectra over a wavelength range from 200 to 800 nm. Quartz cuvettes or 1 mm thick quartz substrates were used for measurements in solution or on thin films, respectively.

Photoluminescence of solid films was studied with a Jobin Yvon-Spex Fluorolog-3 spectrophotometer. Samples were illuminated with a 450 W xenon UV source at an excitation wavelength of 370 nm. Emission spectra from thin film samples were collected in "front-face" mode with spectral resolution of 0.2 nm. For some very thin samples, where the emission was relatively weak, the slit width was increased. This necessitated subtraction of the background substrate emission and rescaling of the emission intensity.

Infrared Spectroscopy. FTIR measurements were performed using an IBM Instruments model IR-32 spectrometer in reflection mode. Spectra were obtained before and after UV irradiation or in situ during electrical operation. The diodes were momentarily turned off during the time that spectra were being recorded since the mechanical force between the electrically biased electrodes is sufficient to distort the polymer layer and prevents proper background correction. Three types of samples were examined: polymer spin-coated onto a gold mirror; polymer on top of an ITO layer deposited on a gold mirror; and in a functioning diode structure with ITO anode and Al cathode. While no electroluminscent emission could be observed from such a diode because of the opacity of the Si and the top Al electrode, similar devices on quartz were prepared and tested electrically. The p-polarized IR beam was incident on the active area of the device through the silicon substrate which was aligned at Brewster's angle to minimize front surface reflection. The Al electrode was thick enough to reflect most of the radiation which therefore passed twice through both the ITO and polymer layers. The configuration of the in situ IR experiment is shown in Figure 1. Such a scheme is possible because of the transparency of silicon and partial transparency of ITO in the IR region. Background measurements were made on control samples with the same ITO and metal thicknesses, but without the polymer layer.

Atomic Force Microscopy. A Park Scientific Autoprobe CP atomic force microscope was used to investigate morphology changes in the polyfluorene films. Since these polymers are rather soft, a nondestructive noncontact mode was employed. Typically the scan size was 1−50 μm^2. No damage due to scanning was evident in the images.

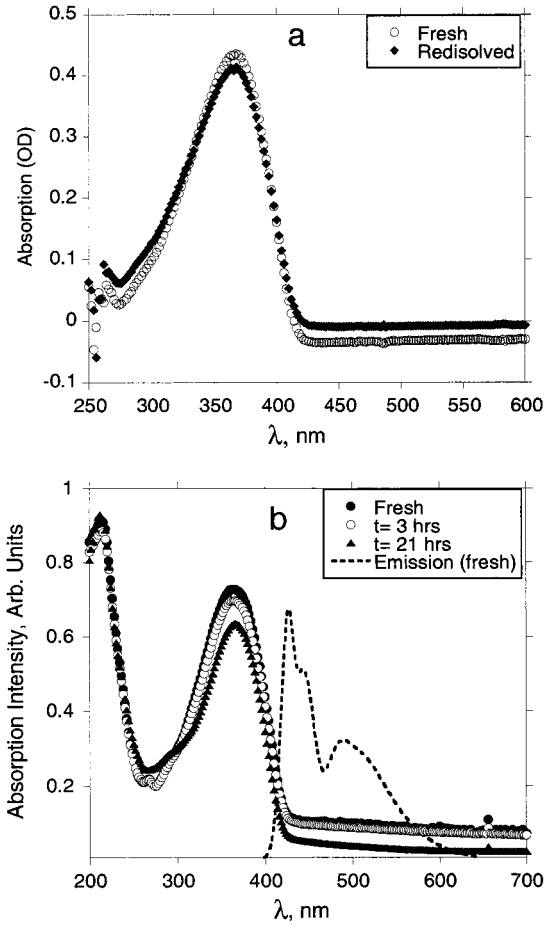

Figure 2. Absorption spectra of PDHF (a) in TCE solution and (b) as a thin films. In part a, we show the absorption spectrum of the original polymer solution (solid diamonds) and of the same sample after casting as a thin film, 6-h UV exposure in air and redissolution (open circles). In part (b) we show the absorption of a 120 nm thick pristine PDHF film (solid circles), the same film after 3 h (open circles), and after 21 h (solid triangles) respectively of UV irradiation in air. The dashed line is the emission spectrum of the fresh film. Neither the solutions nor the films display any dramatic changes in absorption.

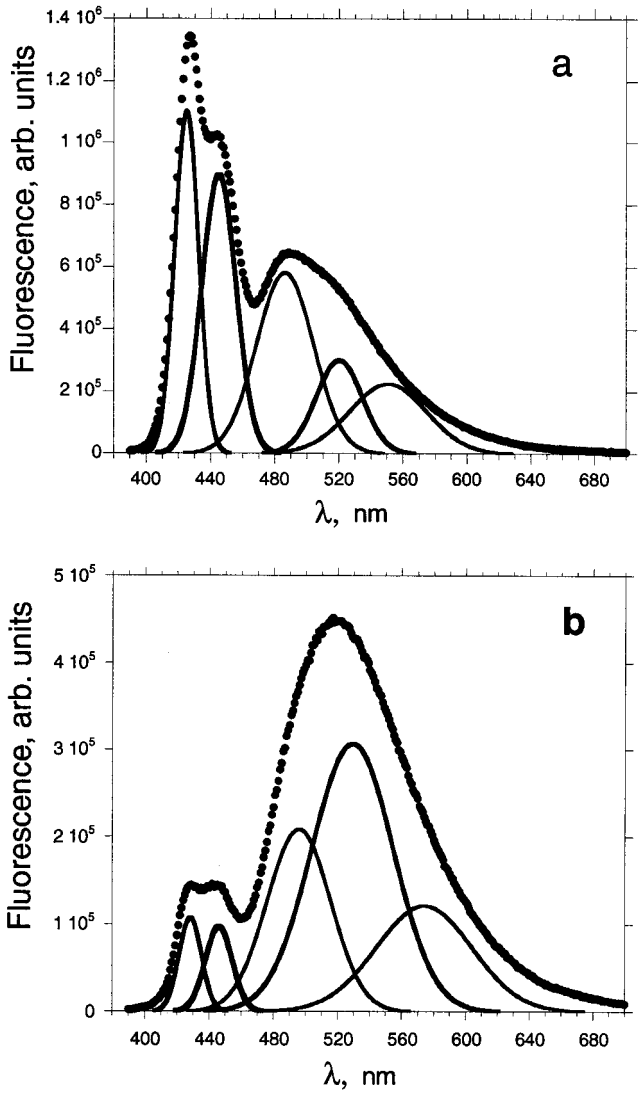

Figure 3. Fluorescence spectra of a 150 nm thick PDHF film (a) before and (b) after 9 h of UV illumination in air. The lines represent the decomposition of the two fluorescent bands into constituent peaks (see text) and show mainly a decrease of the short wavelength (excitonic) band as a result of degradation.

ESCA. The samples used for ESCA experiments were prepared from those used previously for FTIR measurements. With some diode structures, the top Al electrode and most of the polymer film was removed with TCE solvent, exposing the ITO surface with a small amount of polymer residue. In other cases, we peeled apart the layered diode structure using Scotch tape, leaving a thicker layer of polymer attached to the anode. For the samples that had been subjected to UV photodegradation, the air interfaces of the polyfluorene films (on gold or gold/ITO mirrors) were also examined. Analysis was done on a Surface Science Instruments SSX-100 model 5 photoelectron spectrometer with a monochromatic Al K_α source operated in a vacuum at 5×10^{-10} Torr. The absence of charging of the sample surface was checked through the C(1s) aliphatic peak position. The analysis focused primarily on the relative concentrations of oxygen present after various degrees of UV or electrical stress. In addition, the possibility of diffusion of elements from the substrate (In, Sn, Au) through the active layer during functioning of the device was examined.

Experimental Results

Absorption spectra of PDHF both in solution and in thin films are shown in Figure 2. Solution spectra (Figure 2b) are similar to those previously observed.[19] The absorption spectrum in dilute solution has a relatively sharp peak at 380 nm, with an onset of absorption at 430 nm. This position corresponds to a degree of polymerization for PDHF of approximately $n = 10$.[17] The absorption spectrum of a spin-cast film (Figure 2a) is similar except that the peak is broader, reflecting local interactions between neighboring chromophores. Although there is a small amount of bleaching observed with UV irradiation up to 21 h, neither the position of the maximum nor the spectral width changes significantly, implying that the photoinduced degradation does not significantly destroy the conjugated structure.

Figure 3 displays the fluorescence spectra of PDHF films before and after irradiation at 365 nm. Two principal emission bands are observed: at ca. 420 nm and 500−530 nm. Both exhibit fine structure. We ascribe these bands to excitonic emission from noninteracting chains and to excimers resulting from molecular aggregates, respectively.[23−25] In contrast to the absorption spectra, which change very little during irradiation, the band shapes and relative intensities of the emission spectra change dramatically depending on the degradation conditions.

Table 1. Deconvolution of PF Emission Spectra

sample	peak position, nm	assignment
PDHF homopolymer	421 ± 4	exciton (zero phonon)
	444 ± 2	exciton (vibronic)
	491 ± 8	excimer ($N = 2$)
	524 ± 8	excimer ($N = 3$)
	562 ± 11	excimer ($N \geq |4$)
PDHF−15ANT	432 ± 7	exciton (zero phonon)
	448 ± 3	exciton (vibronic)
	464 ± 3	exciton (vibronic)
	498 ± 4	excimer ($N = 2$) or exciton (vibronic)

The fluorescence spectrum of a dilute solution of PDHF (not shown), typical of the isolated polymer chain, shows structure due to vibronic coupling.[26,27] The vibronic spacing is about 1200 cm^{-1}, corresponding to the vibrational levels of the ground-state singlet, S_0. In the solid state (Figure 3), we observe a similar vibronic emission pattern with maxima red-shifted by a few nanometers relative to those in solution.

The second band (500−530 nm) is much broader and results from interchain interactions (excimers) in the solid.[28] Excimers are the result of excitation energy delocalization over two or more neighboring chromophores on different polymer chains which are arranged so that their wave functions overlap. The observed strength of this emission, both in absolute magnitude and relative to the exciton band, is variable and depends on processing conditions and thermal history of the sample. Its relative intensity grows upon annealing and the emission maximum shifts slightly to the red. Analysis of fluorescence spectra of a number of films prepared with different thicknesses, spin-cast from various solvents and with different postdeposition thermal treatment suggests that this band consists of at least three overlapping peaks. Mathematical decomposition of the long wavelength band, assuming Gaussian shapes for all component peaks, reveals a regularity in peak spectral positions. Generally, all the spectra can be reasonably described by three excimer peaks located at 491, 524, and 562 nm. The intensities of the individual components vary from sample to sample changing the overall shape and peak position of this band. We assign these subbands as emission from excimers delocalized over progressively larger aggregates, as detailed in Table 1. Further details are given in the Discussion section.

Turning next to the copolymer, the shape of the PDHF−ANT emission spectra (not shown) both in solution or in films is quite different from that of the homopolymer. The vibronic structure is less well defined and has a smaller splitting (820 cm^{-1}). The excimer band is much weaker or even undetectable in higher molecular weight samples. The exciton band is located at a wavelength where both 9,10-aryl-substituted anthracenes (modeled by 9,10-diphenylanthracene[29]) and the PDHF homopolymer[17] emit. It is therefore difficult to identify the specific chomophore(s) responsible for copolymer emission.

The data of Figures 3 and 4 clearly reveal two different modes of photoinduced degradation in PDHF: one in the presence of oxygen (Figure 3) and the other in an inert nitrogen atmosphere (Figure 4). In the first case, the major changes occur during first 3 h of illumination (see Figure 5) and are characterized by a reduction of both the excitonic (isolated chromophore)

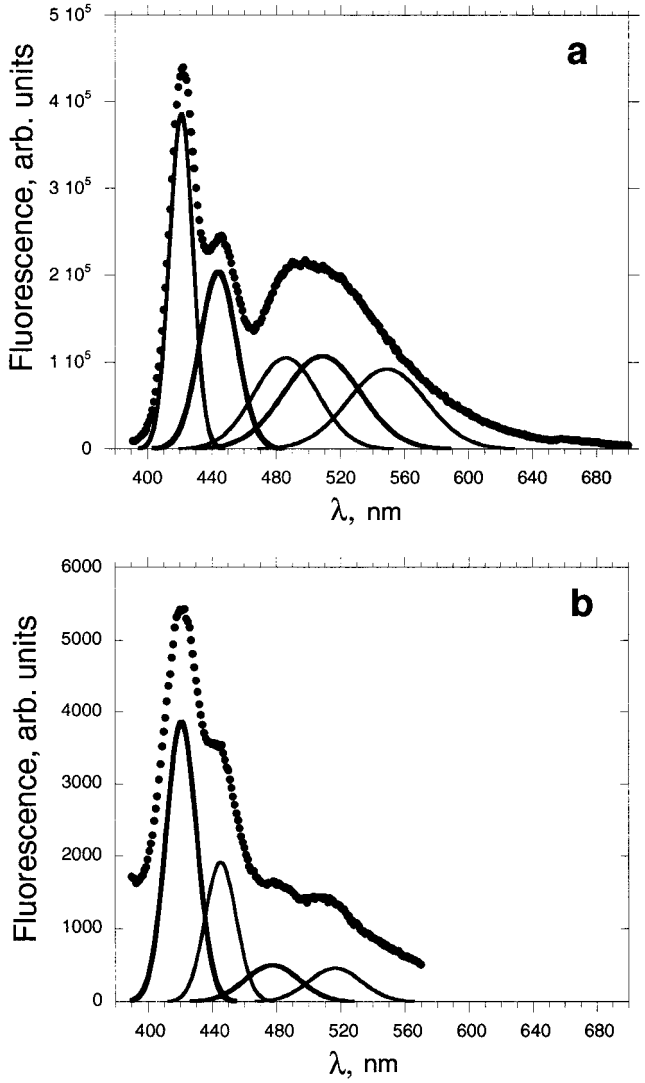

Figure 4. Fluorescence spectra of 120 nm thick PDHF film (a) before and (b) after 15 h of UV illumination in a nitrogen atmosphere. In contrast to the example of photodegradation in air, both emission bands (exciton and excimer) decrease dramatically after irradiation. The relative intensity of the longer wavelength emission (excimer) band is also slightly decreased.

and excimer (aggregate) emission bands. The exciton band decreases more rapidly so that the exciton-to-excimer ratio decreases in time. A different evolution is seen in N_2, where almost no change occurs during the first 6 h of UV irradiation. Upon longer exposure, the excimer band decreases faster and the ratio of exciton to excimer emission increases. Thinner films (<10 nm) show much less excimer emission than those depicted in Figures 3−5, and the degree of aggregation, as monitored by fluorescence, is almost independent of casting solvent.

The effects of electrical degradation on absorption and emission have been studied in a similar way after dissection of failed polymer devices. In-plane PLED fracture always occurs cohesively as revealed by ESCA and AFM studies. The thickness for the polymer film remaining on each electrode, measured by AFM, is about the same (40−60 nm). After electrically degraded devices were peeled apart, PL spectra of both the anode and cathode sides were obtained, as shown in Figure 6. The primary characteristic of the anode (ITO) side is a decreased exciton-to-aggregate ratio similar to that

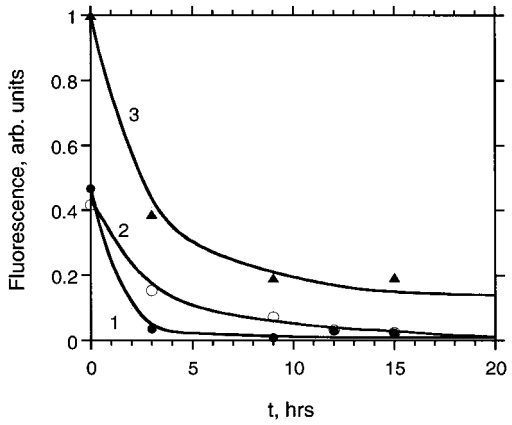

Figure 5. Kinetics of UV degradation of PDHF film in air. Integrated intensities, obtained by spectral deconvolution, of the first 422 nm exciton peak (solid circles), of the first excimer peak at 491 nm (open circles), and of the sum of higher excimer peaks (triangles) versus time of UV illumination at 365 nm. Lines are included as a guide to the eye.

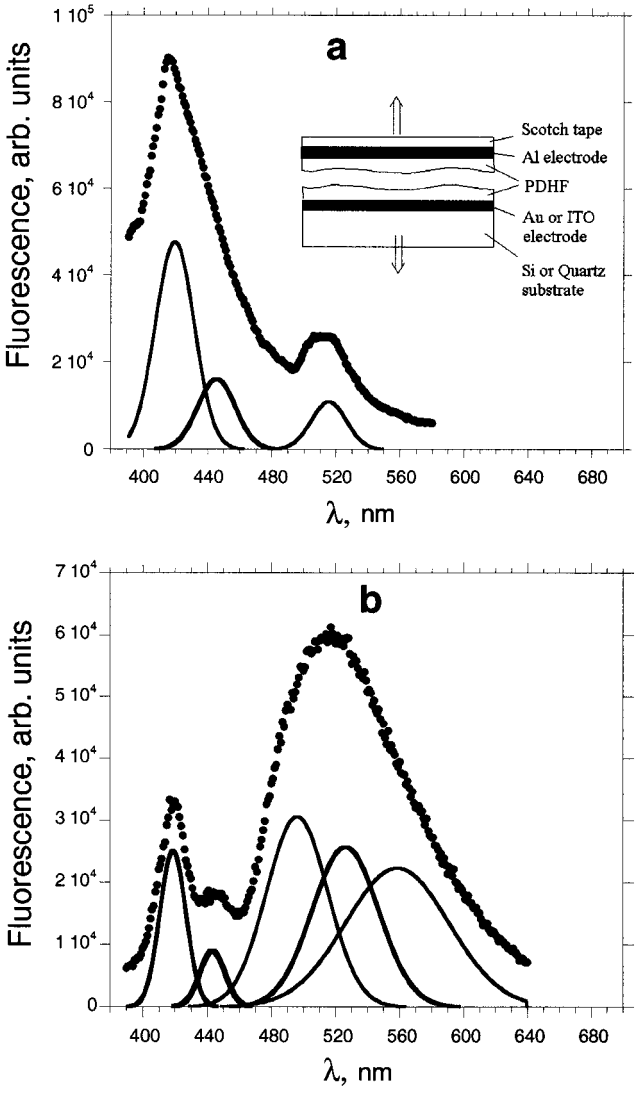

Figure 6. Fluorescence spectra of the PDHF layer after electrical degradation of a working device: (a) the part of the film remaining on the Al cathode; (b) the part remaining on the ITO anode after peeling off the top electrode. The inset illustrates the process of LED device separation.

observed after UV degradation in air (Figure 3). The fluorescence from the cathode (Al) side appears more

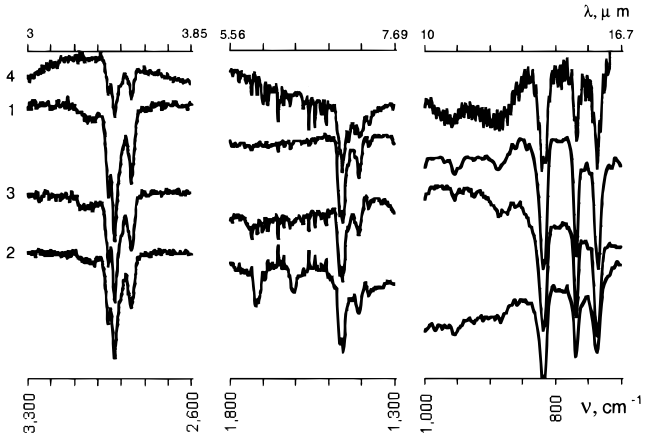

Figure 7. FTIR spectra of (1) a fresh PDHF film, (2) a PDHF film after photodegradation in air, (3) a film after photodegradation in a nitrogen atmosphere and (4) a working LED device, taken in situ, after 1 h at $V = 30$ V, $I = 0.01$A. The most obvious spectral change is the appearance of two new peaks (1717 and 1606 cm^{-1}) occurring only in the case of UV degradation in air.

Table 2. Assignment of Infrared Modes Relevant to Polyfluorenes and Their Degradation

frequency (cm^{-1})	assignment
743−735	fluorene-fluorene rocking and twisting
769−764	out-of-plane bend of four adjacent hydrogens in phenyl (terminal fluorenes)
820−816	out-of-plane bend of 1,2,4-substituted phenyl
885	out-of-plane bend of 1,2,4-substituted phenyl (isolated H in phenyl)
1100	ITO oxygen
1606	asymmetric phenyl semicircular stretch (fluorenone)
1717	C═O stretch in fluorenone

like that of thermally annealed polymer films,[19] but with broader and unresolved constituent peaks.

Chemical changes that occur during and after degradation were also monitored using FTIR spectroscopy. Figure 7 shows the IR transmission spectra of (1) a fresh PDHF film (120 nm), (2) the same film after UV degradation in air, (3) a film exposed to UV under N_2, and (4) a film after operation of a device, with the data obtained in situ. Tentative assignment (Table 2) of the vibrational bands has been made on the basis of previous studies of similar polymers or model compounds[30−32] and by comparison with IR spectra of PDHF−ANT copolymer (not shown in the figure). The bands can be grouped into three main regions, associated with C−H stretching vibrations (around 3000 cm^{-1}), C−H scissoring (at 1600 to 1350 cm^{-1}), and C−H aromatic out-of-plane vibrations (below 850 cm^{-1}), respectively. Several additional very weak peaks between 1350 and 850 cm^{-1} may correspond to overtones and impurities. For PDHF working devices, an additional broad band arising from the ITO is observed at 1100 cm^{-1}.

No changes are observed for the C−H stretching vibrations under any of the degradation conditions. The spectrum of the polymer UV-degraded in N_2 is just a little "noisy" in comparison to the unirradiated sample. The spectra obtained from electrically degraded devices are complicated by the appearance of additional oscillations corresponding to interference of the IR beams

Table 3. X-ray Photoelectron Spectroscopy (ESCA) of PDHF Working LED Devices after Electrically Induced Degradation and of a PDHF Film after UV Degradation in Air

	C(1s)		O(1s)		
sample	energy, eV	concn, at. %[b]	energy, eV	concn, at. %[b]	other[a]
electrically degraded, 40 nm on ITO anode	284	57.3	532.1	0.4	none
	284.5	39.3			
	287.8	0.7			
	290.2	2.3			
		tot.: **99.6**		tot.: **0.4**	
electrically degraded, 20 nm on ITO anode	284.6	83.1	532.2	1.0	traces of Au
	285.4	8.3	533.4	0.6	
	287.6	3.6			
	290.7	3.4			
		tot.: **98.4**		tot.: **1.4**	
electrically degraded, <1 nm on ITO anode	285	52.8	530.3	4.5	In(3p), 5.6 at %; Sn(3d), 0.8 at % from ITO
	286.3	17.7	532.0	4.4	
	287.7	6.1	533.2	1.5	
	288.9	6.5			
		tot.: **83.1**		tot.: **10.4**	
15 h of UV illumination in air	284	74.4	531.5	2.3	none
	284.7	12.4	532.8	3.1	
	287	3.8			
	289.5	4.0			
		tot.: **94.6**		total: **5.4**[c]	

[a] Assignment of the elements in accordance with ref 33. [b] Surface atomic percent compositions calculated from the peak areas with consideration of elemental photoionization cross-sections. [c] 8 at % content of oxygen is expected for two oxygen atoms per fluorene ring of PDHF.

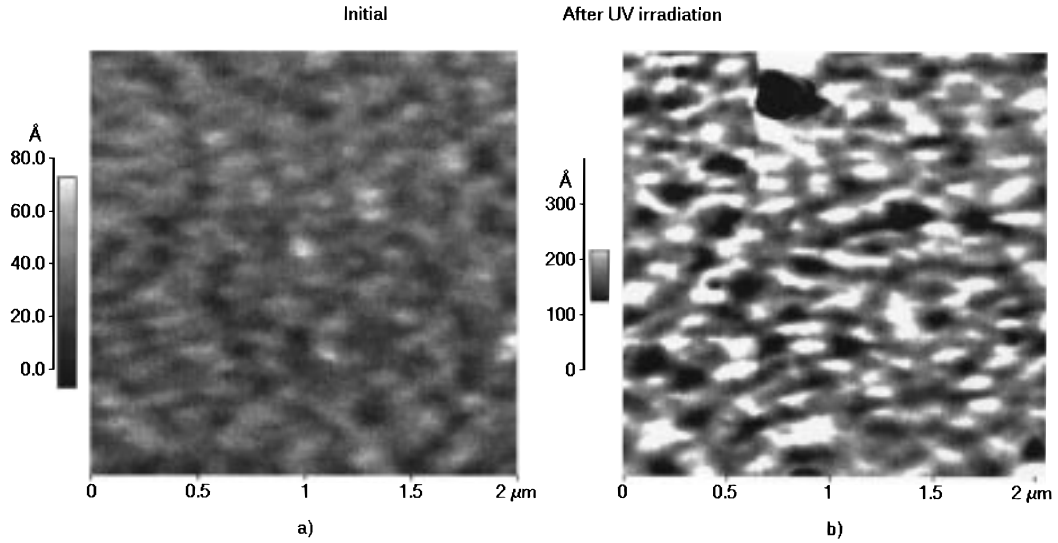

Figure 8. AFM images of the surface of a PDHF film on quartz (a) before and (b) after UV degradation in air showing a 3-fold increase in rms roughness.

reflected from the front and the back sides of the device.[31]

The most obvious changes in the IR spectra of degraded samples are observed in the fingerprint region (1800−600 cm^{-1}), but only in the case of UV degradation in air are the spectroscopic changes well pronounced. In these samples, two new bands appear at 1717 and 1606 cm^{-1}. The latter may be interpreted as a stretching mode of an asymmetrically substituted benzene ring whereas the former is consistent with the carbonyl stretch of an aromatic ketone or ester.[31,32] The intensities of these two peaks increase with the UV fluence and clearly result from photooxidation. In each case, the changes in the shape of the baseline suggest that the film morphology is also affected by the degradation process (vide infra).

Results of ESCA analysis[33] on samples degraded electrically and by UV exposure in air are summarized in Table 3. The latter treatment results in considerable increase in oxygen content, corresponding to nearly one O atom for every two fluorene monomer units. Since there are no corresponding changes in the IR spectra, for example no C−O, C−O−C, or OH bands, we attribute the high level of O to the surface selectivity of ESCA. In the case of the thinnest sample prepared after electrical degradation, some of the oxygen signal can be attributed to the ITO electrode. In the thicker samples (20 and 40 nm) there is no evidence, at the 0.5% atomic detection limit, of indium or tin diffusion into the polymer. Devices peeled apart without running show no detectable oxygen.

The surface morphology of the PDHF films were studied by AFM. Figure 8 shows the surface of a PDHF film before and after UV irradiation in air. A pronounced increase of the rms roughness (from 1 to 3 nm over a 1 × 1 μm^2 area) is determined from the

captured images. Almost no changes were observed in surface roughness of the sample exposed to UV in nitrogen.

Discussion

An excited chromophore can return to the ground state by a number of pathways involving both intermolecular and intramolecular interactions. However, while the system is in the excited state both physical (reorientation, diffusion, aggregation) and chemical (isomerization, dissociation, oxidation) changes may occur. Two major photochemical processes, oxidation and crosslinking, can alter the chemical structure of the original chromophore and cause a permanent change in both absorption and fluorescence. Since the chemical products of these processes may also enhance nonradiative relaxation rates, for example by creating quenching centers, they often tend to reduce the quantum efficiency of electroluminescence.[34] In our case, the fluorescence results (Figures 3, 4, and 6) suggest that two different mechanisms of degradation occur in the system, namely one that rapidly decreases both exciton and excimer emission, as well as the exciton/excimer ratio, and another which has a lesser effect on the total emission but increases the exciton/excimer ratio. The first of these, which we term "the photochemical mechanism", occurs in the presence of oxygen and is associated with the appearance of carbonyl bands in the IR spectra and an enhanced oxygen signal in the ESCA spectra. The chemical changes are thus clearly oxidative in nature. The second mechanism provides no distinctive signatures by any analytical technique other than fluorescence. It is reasonable, therefore, to suggest that the second mechanism should be described in terms of morphological changes which promote energy loss through exciton migration and enhanced quenching in aggregates.

Chemical Degradation (Oxidation). The appearance of two IR new peaks (1717 and 1606 cm^{-1}) are suggestive of oxidation to fluorenone-containing structures, fluorenone itself having strong bands at 1708 and 1600 cm^{-1}. Most likely, the terminating fluorene monomers, having hydrogens at the 9-position, are the primary sites for this oxidation mechanism. This scenario is consistent with the absence of any noticeable changes in the UV−vis absorption spectra indicating that little chain scission occurs as a result of oxidation (Figure 2b). It is also accounts for the lack of changes in the C−H stretching bands and aromatic out-of-plane vibrations. The severe suppression of the exciton luminescence band (Figure 3b) is then explained in terms of exciton diffusion to the fluorenone quenching centers. The excimer emission is less affected because excimers are less mobile. More detailed studies, using different end groups, are required to prove conclusively that end-group oxidation is the primary photooxidation process in PDHF. It also remains to be shown that fluorenone units can act as quenching centers.

The observed morphological changes of PDHF films subjected to photodegradation in air may be explained as follows. The amorphous polymer film has sufficient free-volume to allow the diffusion of oxygen. The bulk of the material is oxidized at random, causing local changes in chain conformation and packing density. As a result the surface is roughened.

The absence of chemical oxidation in LED devices is worth noting. In contrast to the case of PDHF exposed to UV light in air, there is no appearance of a carbonyl band in the IR. Furthermore, ESCA analysis (Table 3) shows only very minor changes in the oxygen content of electrically degraded polymer films. The largest change occurs close to the ITO electrode, and some of this may be attributed to oxygen in ITO itself. These data may be compared with previously reported electrical degradation studies of MEH−PPV[14] in which the ITO electrode was recognized as a reservoir of oxygen for the oxidation of the polymer layer. In that case, there was a clear carbonyl signature in the IR spectra of electrically aged devices. These results confirm that polyfluorenes are considerably more oxidatively stable than phenylene vinylenes.

Physical Degradation (Excimers and Quenching). In the absence of oxygen, the changes in fluorescence are not accompanied by evidence for chemical changes in the polymer. We are led, therefore, to consider a mechanism involving physical/structural processes. Excimers are known to provide nonradiative relaxation pathways which lead to reduced emission efficiency relative to exciton luminescence. Therefore in this section, we discuss the role of excimers and propose a degradation mechanism involving aggregate growth. It was shown by time-resolved luminescence studies[35] that transport of mobile excitations to randomly distributed quenching centers[34] could be responsible for nonradiative recombination in conjugated polymers. The nature of such nonradiative defect(s) is not always known. Frequently, oxygen or oxygen-containing fragments (e.g., carbonyl) act as electron traps and efficient quenching defects. Here we consider physical quenching in stacks of planar chromophores, a process which is well-known for many organic dyes and aromatic molecules (e.g., anthracene, perylene, pyrene, etc.).[29]

Excimers are formed by interaction of an excited chromophore with an unexcited neighbor(s), forming a more delocalized, and therefore lower energy, excited-state complex. Stabilization occurs via resonance contributions from exciton and charge-transfer configurations.[36,37] Structural studies of many π-conjugated small-molecule chromophores have shown that their basic supramolecular structures in the solid are cofacial stacks. Since conjugated polymers often possess rigid chains with relatively planar geometries and substantial intermolecular interactions, they are prone to form similar cofacial structures (dimers and other aggregates) in the solid,[38] facilitating the formation of excimers in the excited state.

In accordance with the molecular exciton approximation proposed by Kasha et al.[21] based on the molecular exciton theory of Davidov,[39] the energy shift between the isolated chromophore band and N-chain aggregate is given as follows:

$$\Delta E = E_a - E_s = 4\left[\frac{(N-1)}{N}\frac{\langle M\rangle^2}{r^3}(\cos\alpha - 3\cos^2\theta)\right] \quad (1)$$

Here E_a is the (excimer) transition energy for an assembly of N chromophores, E_s is that of the isolated single chromophore, $\langle M\rangle^2$ is the square transition dipole moment of the single chain, r is the center-to-center distance between participating chromophores, α is the torsion angle, and θ is the tilt angle between the moments. The relative shifts of the excimeric components from the main (excitonic) peak at 422 nm in

polyfluorenes are in a good agreement with this expression, which predicts relative shifts of different aggregate bands in proportion: (1/2):(2/3):(3/4):...: $(N - 1/N)$. The maximum shift is observed for "infinite" N and the dimer is exactly halfway between the exciton and the large N limit. Such behavior is experimentally observed in the absorption of ground-state aggregates and in some cases in the emission spectra of chromophore-containing systems.[22] Application of the model to our case suggests the presence of pairs, triads and unresolved larger values of N present in different proportions in PDHF films. It should be emphasized that the size of the elementary chromophore is approximately 10 monomer units (the entire length of our PDHF oligomers[17]) and the aggregates consist of assemblies of these chains. Although the physical size and the number of chromophores per aggregate may be large, the spectroscopic and other electronic properties of the excimer are determined by the effective or spectroscopic aggregation number N in eq 1. It is worth emphasizing that there is no evidence for ground-state interactions between polymer chains; the absorption spectra of dilute solutions and solid films are very similar.

Fluorene polymers, which can be described as rigid rods, are prone to form nematic-type packing in the bulk.[40] Such a structural organization explains the optical features observed here. Indeed, nematic structures are characterized by an orientational order parameter (side-by-side arrangement of high aspect ratio molecules with no correlation in longitudinal position). Equation 1 therefore predicts a red-shifted emission ($\theta < 54.7°$) corresponding to the interaction of π-orbitals in slipped planar arrangements of neighboring molecules. The most probable alignment is one in which half of the monomers (5) in each pair overlap. Assuming that the transition dipole is aligned along the molecular axis, the angle $\theta \sim 5°$. Moreover the mean value of α is zero. The remaining parameters in eq 1 can, in principle, be determined from quantitative analysis of the emission spectrum.[22,41] However, this is very difficult in this case, because of the wide range of probabilities for the formation of different overlapping aggregate structures, ranging from 1 to 10 monomeric units. As a result, the emission band due to pairs, as well as of those from higher aggregates, is severely broadened.

Geometrical aggregates may be additionally perturbed by the packing of the six-carbon aliphatic substituent groups. In fact, this process may be responsible for the lower exciton-to-excimer ratio in very thin films, due to surface dominated morphology. Because of different surface energies of the conjugated PDHF chain and the aliphatic side groups, the latter may dominate near the surface, resulting in a more smectic than nematic liquid crystalline ordering.

The term "excimer" refers to a bound state that exists only in the excited state whereas the ground state of the complex is dissociated.[28] We have assigned the long-wave emission to excimers rather than ground-state aggregates[23] on the basis of two observations. First, as discussed above, there is no change in the absorption spectra associated with the growth of the long wavelength emission band. Second, the excitation spectrum of the long wavelength bands is the same as that for the excitonic band. Therefore we conclude that the red-shifted emission occurs through excited state complexation, requiring only small changes in the relative positions of neighboring chains. It should be noted however, that a favorable initial molecular geometry is required for excimer formation in the solid, such that minimal reconstruction occurs in the excited-state binding of the chromophores. (The glass transition temperatures of the polymers studied are all above 100 °C.) Thus, partial orientation through local nematic ordering would favor excimer formation.

In an amorphous material with a distribution of excitation energies, any exciton will tend to migrate to progressively lower energy sites.[42] Thus an exciton initially excited on a single chromophore in the polymer chain may diffuse to an aggregate where the energy is lower due to excimer stabilization. In such a case, not only is the energy of emission shifted to longer wavelength, but also the quantum yield is generally reduced due to the availability of additional nonradiative pathways through coupling to the additional vibrational degrees of freedom in the excimer.[43]

In the case of electrical excitation, excimers can also be formed through recombination of injected positive and negative charges[37] to form first an exciton which then migrates to a site favorable for excimer formation. Thus one might expect similar mechanisms for oxygen-free photo- and electrical degradation.

We propose a scenario which may be responsible for the physical process leading to changes in the emission spectra (Figure 4), namely, enhanced aggregation as a direct result of excimer formation. The accumulation of many small molecular motions which occur due to excimer binding leads to a progressive growth and alignment of aggregates. The larger and more ordered aggregate regions then tend to trap and quench the energy of the exciton population. The excimers become progressively delocalized over an increasing number of chromophores which further lowers the quantum yield. Thus both the exciton and excimer peaks in the emission spectrum are quenched (Figure 4b) and the decrease in emission is relatively more complete in the excimer region. Since the growing aggregates still constitute only a very small fraction of the polymer film, this mechanism does not necessarily lead to noticeable changes the absorption spectrum or surface roughness. The physical nature of the degradation is further revealed by an experiment in which material from a UV/N_2 exposed film was redissolved and used to cast a new sample. The initial emission spectrum was recovered and the luminescent efficiency returned to approximately 70% of the pristine film. When the UV exposure was conducted in air the spectral changes were permanent. The proposed mechanism also explains the higher stability observed in the PDHF−15ANT copolymer, which is not prone to excimer formation even upon extended thermal annealing.[18] Aggregate formation is inhibited by steric interactions and hence there is no aggregate-related fluorescence quenching.

Aggregate growth in the homopolymer may occur simultaneously with photochemical oxidation, but its effects would be overwhelmed. Direct structural observations are needed to prove changes in aggregate fraction, and reveal the differences between the homo- and copolymers.

Conclusions

The studies described in this paper reveal that the stability of polyfluorene polymers against photoinduced and electrical degradation is much higher than that of PPV-type polymers. The stability of the fluorenes under

UV irradiation in an inert atmosphere is about an order of magnitude greater than in air. Two primary scenarios of degradation, one chemical and one physical, have been identified.

In the chemical route, oxidation of the polymer leads to the formation of carbonyl containing species, postulated as fluorenones, which quench the fluorescence. Oxidative degradation of these polymers electrically in working devices is not observed. Additional improvement in oxidative stability should be achievable by careful choice of end-group substituents. The oxidative degradation process is manifested by a fluorescence intensity shift from the blue exciton emission to the green excimer band because excitons diffuse to the carbonyl quenching centers, whereas excimers are essentially immobile.

The physical process involves exciton migration to sites capable of forming excited state aggregates. These regions grow in number and/or size through localized molecular motions and induce more nonradiative relaxation through excimer formation. The physical process is characterized by decreased emission intensity and only minor changes in the relative intensities of the two emission bands. The physical stability is improved by inhibiting aggregate formation, for example in very thin films or by using steric hindrance to prevent face-to-face packing of chromophores, as in the fluorene-anthracene copolymer, PDHF−15ANT.

Acknowledgment. We thank Jesse Salem and Bruce Melior for their help with FTIR experiments. V.N.B. acknowledges support from the Packard Foundation. This work was supported in part by the NSF (Grant DMR-9704177), and by the Center on Polymer Interfaces and Macromolecular Assemblies (CPIMA, NSF Grant No. DMR-9400365).

References and Notes

(1) Burroughes, J. H.; Bradley, D. D. C.; Brown, A. R.; Marks, R. N.; Mackey, K.; Friend, R. H.; Burns, P. L.; Holmes, A. B. *Nature* **1990**, *347*, 539.
(2) Yang, Y. *MRS Bull.* **1997**, 31.
(3) Braun, D.; Heeger, A. J. *Appl. Phys. Lett.* **1991**, *58*, 1982.
(4) Bradley, D. D. C. *Synth. Met.* **1993**, *54*, 401.
(5) Berggren, M.; Inganas, O.; Gustafsson, G.; Rasmusson, J.; Andersson, M. R.; Hjertberg, T.; Wennerstrom, O. *Nature* **1994**, *372*, 444.
(6) Faraggi, E. Z.; Chayet, H.; Cohen, G.; Neumann, R.; Avny, Y.; Davidov, D. *Adv. Mater.* **1995**, *7*, 742.
(7) Tasch, S.; List, E. J. W.; Hochfilzer, C.; Leising, G.; Schlichting, P.; Rohr, U.; Geerts, Y.; Scherf, U.; Mullen, K. *Phys. Rev. B.* **1997**, *56*, N8, 4479.
(8) Gruner, J.; Hamer, P. J.; Friend, R. H.; Huber, H.-J.; Scherf, U.; Holmes, A. *Adv. Mater.* **1994**, *6*, 748.
(9) Huber, J.; Mullen, K.; Salbeck, J.; Schenk, H.; Scherf, U.; Stehlin, T.; Stern, R. *Acta Polym.* **1994**, *45*, 244.
(10) Pei, Q.; Yang Y. *J. Am. Chem. Soc.* **1996**, *118*, 7416.
(11) Sheats, J. R.; Antoniadis, H.; Hueschen, M.; Leonard, W.; Miller, J.; Moon, R.; Roitman, D.; Stocking, A. *Science* **1996**, *273*, 884.
(12) Rabek, J. F. *Photodegradation of Polymers. Physical Characteristics and Applications*; Springer: Berlin, 1996.
(13) Scurlock, R. D.; Wang, B.;. Ogilby, P.R; Sheats, J. R.; Clough, R. L. *J. Am. Chem. Soc.* **1995**, *117*, 10194.
(14) Scott, J. C.; Kaufman, J. H.; Brock, P. J.; DiPietro, R.; Salem, J.; Goitia, J. A. *J. Appl. Phys.* **1996**, *79*, 2745.
(15) Fukuda, M.; Sawada, K.; Yoshino, K. *J. Polym. Sci., Part A: Polym. Chem.* **1993**, *31*, 2465.
(16) Grell, M. M.; Bradley, D. D. C.; Inbasekaran, M.; Woo, E. P. *Adv. Mater.* **1997,** *9*, 798.
(17) Klaerner, G.; Miller, R. D. *Macromolecules* **1998**, *31*, 2007.
(18) Kreyenschmidt, M.; Klaerner, G.; Fuhrer, T.; Ashenhurst, J.; Karg, S.; Chen, W. D.; Lee, V. Y.; Scott, J. C.; Miller, R. D. *Macromolecules* **1998**, *31*, 1099.
(19) Klärner, G.; Davey, M. H.; Chen, W. D.; Scott, J. C.; Miller, R. D. *Adv. Mater.* **1998**, *10*, 993.
(20) Yamamoto, T.; Morita, A.; Muyazaki, Y.; Maruyama, T.; Wakayama, H.; Zhou, Z.-H.; Nakamura, Y.; Kanbara, T.; Sasaki, S.; Kubota, K. *Macromolecules* **1992**, *25*, 1214.
(21) Kasha, M.; Rawals, H. R.; Ashraf El-Bayoumi, M. *Pure Appl. Chem.* **1965**, *11*, 371.
(22)) Sauer, T.; Caseri, W.; Wegner, G. *Mol. Cryst. Liq. Cryst.* **1990**, *183*, 387.
(23) Lemmer, U.; Heun, S.; Mahrt, R. F.; Scherf, U.; Hopmeier, M.; Siegner, U.; Gobel, E. O.; Mullen, K.; Bassler, H. *Chem. Phys. Lett.* **1995**, *240*, 373.
(24) Osaheni, J. A.; Jenekhe, S. A. *Macromolecules* **1994**, *27*, 739.
(25) Harigaya, K. *Chem. Phys. Lett.* **1997**, *281*, 319.
(26) McRae, E. G. *Austr. J. Chem.* **1961**, *14*, 354.
(27) McClure, D. S. *Can. J. Chem.* **1958**, *36*, 59.
(28) Birks, J. B. *Rep. Prog. Phys.* **1975**, *38*, 903.
(29) Berlman, I. B. *Handbook of Fluorescence Spectra of Aromatic Molecules*, 2nd ed.; Academic Press: New York, 1971.
(30) Fukuda, M.; Sawada, K.; Yoshino, K. *J. Polym. Sci., Polym. Chem.* **1993**, *31*, 2465.
(31) *Fourier Transform Infrared Spectroscopy. Applications to Chemical Systems*, Vol.4; Ferraro, J. R.; Basile, L. J., Eds.; Academic Press: Orlando, Fl, 1985.
(32) *The Aldrich Library of Infrared Spectra Edition III*; Pouchert, C. J., Ed.; Aldrich Chemical Co., Inc.: Milwaukee, WI, 1981.
(33) *Handbook of X-ray Photoelectron Spectroscopy*; Wagner, C. D.; Riggs, W. M.; Davis, L. E.; Moulder, J. F.; Muilenberg, G. E., Eds.; Perkin-Elmer Corporation: Norwalk, CT, 1979. Scofield, J. H. *J. Electron Spectrosc.* **1976**, *8*, 129.
(34) Yan, M.; Rothberg, L. J.; Papadimitrakopoulos, F.; Galvin, M. E.; Miller, T. M. *Phys. Rev. Lett.* **1994**, *73*, 744.
(35) Lemmer, U.; Mahrt, R. F.; Wada, Y.; Greiner, A.; Bassler, H.; Gobel, E. O. *Appl. Phys. Lett.* **1993**, *62*, 2827.
(36) Jenekhe, S. A. *Adv. Mater.* **1995**, *7*, 309.
(37) Jenekhe, S. A.; Osaheni, J. A. *Science* **1995**, *265*, 765.
(38) *Liquid crystalline polymers*; Donald A. M.; Windle, A. H., Eds.; Cambridge University Press: Cambridge, New York, 1992.
(39) Davydov, A. S. *Theory of Molecular Excitons*; Plenum Press: New York, 1971.
(40) Bradley, D. D. C.; Grell, M.; Grice, A.; Tajbakhsh, A. R.; O'Brien, D. F.; Bleyer, A. *Opt. Mater.* **1998**, *9*, 1.
(41) Fujiki, M.; Tabei, H.; Kurihara, T. *J. Phys. Chem.* **1988**, *92*, 1281.
(42) Yamazaki, I.; Tamai, N.; Yamazaki, T. *J. Phys. Chem.* **1990**, *94*, 516.
(43) Mooney, W. F.; Whitten, D. G. *J. Am. Chem. Soc.* **1986**, *108*, 5712.

MA9808979